FINITE ELEMENT COMPUTATION OF FIELD, LOSSES AND FORCES IN A THREE-PHASE GAS CABLE WITH NON-SYMMETRICAL CONDUCTOR ARRANGEMENT

D.Labridis P.Dokopoulos

Power Systems Laboratory

Aristotelian University of Thessaloniki , Greece

Keywords: Gas cables, finite element method, eddy currents, losses, inductances, forces.

Abstract - This paper presents a finite element field computation in a three phase gas insulated power cable. The phase conductors carry sinusoidal currents in a steady-state and balanced condition. Both symmetrical and non-symmetrical conductor arrangements are examined, taking into account the real geometrical and physical cable properties. Losses, forces, inductances and current density distribution are calculated. Comparison is made with theoretical and experimental results given in the literature.

1. Introduction

Easy construction, good heat transfer through the dielectric, low losses and inexpensive terminations are some of the advantages of the gas insulated cables. They are now used for the transmission of high electrical power and in SF_6 insulated substations.

Calculation of field, losses and forces are of importance for the design and reasonable operation of the transmission system. The first attempts for calculations were made by approximating the complex cable geometry. The phase conductors were replaced by flat, infinitesimally thin sheets [1] or with curvilinear trapeziums [2] or with zero thickness tubes [3] . Also the enclosure was assumed to be extended to infinity [1], [2] . Another model [4] has taken into account the real geometry introducing four ficticious current sheets.

The approximating models did not allow the evaluation of the current density distribution inside the conductors and inside the enclosure. The investigations were also limited to symmetrical conductor arrangements.

The purpose of this work is the analysis of field, current density distribution, losses, inductances, forces and flux density equipotentials for the general non-symmetrical arrangement.

A general-purpose finite element computer program has been developed treating the quasi-static current density [5] or the so called source current density in each conductor as an unknown. The given quantity is the rms measurable current flowing through each conductor. By solving a coupled system of differential and algebraic equations, the vector potential and the current density are determined. All the other performance quantities are easily obtained from the finite element solution, using symmetric quadrature formulae [6] .

The results have been compared with analytical solutions [1] , [2] , [4] and with measurements [7] . Agreement with the measurements and with the more accurate representation of [4] was excellent.

88 WM 131-5 A paper recommended and approved by the IEEE Insulated Conductors Committee of the IEEE Power Engineering Society for presentation at the IEEE/PES 1988 Winter Meeting, New York, New York, January 31 - February 5, 1988. Manuscript submitted June 24, 1987; made available for printing November 13, 1987.

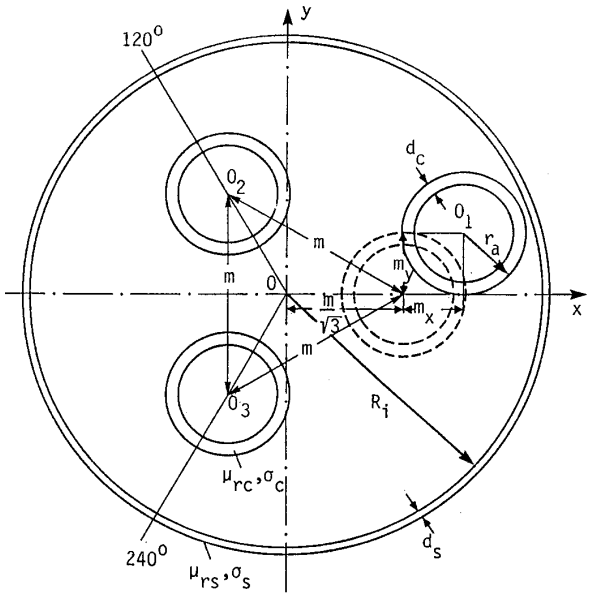

Fig. 1. Cross section of the cable

2. The model

The cable consists of three tubular phase conductors non-symmetrically arranged within a tubular shell as shown in Fig. 1.

The following assumptions are made:

1) The cable is infinitely long, so that the problem becomes a two-dimensional one.
2) Charges and displacement currents are neglected.
3) The conductors and the sheath have constant conductivities and relative permeabilities.
4) The phase currents are sinusoidal and balanced.

Based on the last assumption the following complex functions for the time variation of the three conductor currents are introduced

$$\tilde{I}_1 = \sqrt{2}\, I_{rms}\, e^{j\omega t}$$
$$\tilde{I}_2 = \sqrt{2}\, I_{rms}\, e^{j(\omega t - 2\pi/3)} \qquad (1)$$
$$\tilde{I}_3 = \sqrt{2}\, I_{rms}\, e^{j(\omega t - 4\pi/3)}$$

where I_{rms} is the only measurable quantity in the cable.

3. The electromagnetic field equations

The assumptions made lead to a linear, steady-state, time harmonic electromagnetic field which is governed by Maxwell's equations

$$\nabla \times \vec{H} = \vec{J} \qquad (2)$$

0885-8977/88/1000-1326$01.00©1988 IEEE

$$\nabla \times \vec{H} = - j\omega\vec{B} \tag{3}$$

$$\nabla \cdot \vec{B} = 0 \tag{4}$$

Ohm's law at a point

$$\vec{J} = \sigma\vec{E} \tag{5}$$

the continuity relation

$$\nabla \cdot \vec{J} = 0 \tag{6}$$

and the constitutive relation

$$\vec{B} = \mu_o\mu_r \vec{H} \ . \tag{7}$$

Introducing the magnetic vector potential with curl

$$\nabla \times \vec{A} = \vec{B} \tag{8}$$

and divergence, according to Coulomb's gauge

$$\nabla \cdot \vec{A} = 0 \tag{9}$$

(3) becomes

$$\nabla \times (\vec{E} + j\omega\vec{A}) = 0 \tag{10}$$

Since the curl of the expression in the parentheses in (10) equals zero, it must be equal to the gradient of a scalar function φ, thus

$$\vec{E} + j\omega\vec{A} = - \nabla\varphi \tag{11}$$

If the electric scalar potential is taken to be this scalar function, (11) satisfies the requirements for both static and time-varying situations.

Using (2), (7), (8) and (11) the linear diffusion equation is derived as follows

$$\frac{1}{\mu_o\mu_r} (\nabla\times\nabla\times\vec{A}) = -j\omega\sigma\vec{A}-\sigma\nabla\varphi \tag{12}$$

The current density J is now separated into two components

$$\vec{J} = \vec{J}_e + \vec{J}_s \tag{13}$$

where $\vec{J}_e$ is related to the variation of the magnetic vector potential, called eddy current density and $\vec{J}_s$ is related to the gradient of the electric scalar potential, called source current density. (5) and (11) lead to

$$\vec{J} = -j\omega\sigma\vec{A} - \sigma\nabla\varphi \tag{14}$$

so that

$$\vec{J}_e = - j\omega\sigma\vec{A} \tag{15}$$

and

$$\vec{J}_s = - \sigma\nabla\varphi \ . \tag{16}$$

Supposing the current density vector is in the $\hat{z}$ direction, the two-dimensional diffusion problem is described by the system of equations

$$\frac{1}{\mu_o\mu_r} \left(\frac{\partial^2 A}{\partial x^2} + \frac{\partial^2 A}{\partial y^2} \right) - j\omega\sigma A + J_s = 0 \tag{17a}$$

$$-j\omega\sigma A + J_s = J \tag{17b}$$

and the appropriate boundary relations, that are the continuity of the normal components of the flux density B and the continuity of the tangential components of the magnetic field H across the boundary between two media.

In equation (17) A and J_s are the unknowns and J is specified in the integral form

$$\iint_S J \, ds = I_{rms} \tag{17}$$

where I_{rms} is the measurable current flowing in a conductor of cross-section S.

4. Finite element formulation

It has been shown [8] that for a straight conductor the source current density J_s is constant over its cross-sectional area. So the unknowns A and J_s are approximated in terms of linear interpolation polynomials N(x, y) and N_s(x, y) (see Appendix I) as

$$A(x, y) = \mathbf{N}^T\mathbf{A} \tag{18a}$$

$$J_s(x, y) = \mathbf{N}_s^T \mathbf{J}_s \tag{18b}$$

where, in a problem with M nodes and N conductors,

$$\mathbf{A}^T = \begin{bmatrix} A_1 & A_2 & \dots & A_M \end{bmatrix} \ , \ \mathbf{J}_s^T = \begin{bmatrix} J_{s1} & J_{s2} & \dots & J_{sN} \end{bmatrix} , \tag{19a}$$

$$\mathbf{N}^T = \begin{bmatrix} N_1 & N_2 & \dots & N_M \end{bmatrix} \ , \ \mathbf{N}_s^T = \begin{bmatrix} 1 & 1 & \dots & 1 \end{bmatrix} . \tag{19b}$$

Applying the Galerkin method to the system of equation (17) and assembling in the usual way [5] the element contributions, leads to the following matrix equation

$$\begin{bmatrix} \frac{1}{\mu_o\mu_r}\mathbf{S} - j\omega\sigma\mathbf{T} & -j\omega\sigma\mathbf{Q} \\ -j\omega\sigma\mathbf{Q}^T & j\omega\mathbf{W} \end{bmatrix} \begin{bmatrix} \mathbf{A} \\ \mathbf{G} \end{bmatrix} = \begin{bmatrix} \mathbf{0} \\ \mathbf{I} \end{bmatrix} \tag{20}$$

where $\mathbf{S}$ and $\mathbf{T}$ are the usual finite element square matrices encountered in the solution of eddy current problems [10] and

$$\mathbf{Q}^T = \begin{bmatrix} q_1 & q_2 & \dots & q_N \end{bmatrix}, \quad \text{where } q_i = \iint_{S_i} N dS \ , \tag{21a}$$

$$\mathbf{I}^T = \begin{bmatrix} I_1 & I_2 & \dots & I_N \end{bmatrix}, \quad \text{where } I_i = \iint_{S_i} J dS \ , \tag{21b}$$

$$\mathbf{W} = \text{diag}\begin{bmatrix} w_1 & w_2 & \dots & w_N \end{bmatrix}, \quad \text{where } w_i = \iint_{S_i} dS = S_i \ , \tag{21c}$$

S_i is the area of the cross-sectional surface of conductor i and

$$\mathbf{G} = \frac{1}{j\omega\sigma} \mathbf{J}_s \ . \tag{21d}$$

The total coefficient matrix in (20) is symmetrical of order M+N, with M unknown nodal vector potentials A_i and N unknown conductor sourse current densities J_{si}.

Due to the special structure of the matrix in (20) the conventional band solutions are not effective. Nevertheless care has been taken to reduce the bandwidth of the upper left sub-matrix with automatic node renumbering. Further storage requirement reduction has been accomplished by storing and computing only within the non-zero profile of the equations. The Crout variation [9] of Gauss elimination has been used to obtain a direct solution of (20).

The cable domain has been discretized into 3057 triangles with 1534 nodes. The total coefficient matrix has been reduced to a vector with about 160000 non-zero terms.

It is of interest that in the discretization of the sheath the physical properties of the material have been considered. So the discretization was a function of the skin depth δ_s of the sheath. This led into a better approximation of the current density decay and of the tangential boundary relation.

5. Losses

In the general non-symmetrical arrangement the ac losses per unit lenght of the cable are

$$P_t = P_{c1} + P_{c2} + P_{c3} + P_s \quad . \tag{22}$$

Defining an ac resistance such as

$$P_t = 3\, I^2_{rms}\, R_{ac} \tag{23}$$

the ac/dc ratio will be

$$\frac{R_{ac}}{R_{dc}} = \frac{1}{3}\left(\frac{P_{c1}}{P_{dc}} + \frac{P_{c2}}{P_{dc}} + \frac{P_{c3}}{P_{cd}}\right) + \frac{P_s}{3P_{dc}} \quad . \tag{24a}$$

In the symmetrical case the ac/dc ratio becomes

$$\frac{R_{ac}}{R_{dc}} = \frac{P_c}{P_{dc}} + \frac{P_s}{3P_{dc}} \quad . \tag{24b}$$

From the solution of the system in (20) it is possible to calculate both sides of (24) and therefore to make a verification.

A complex voltage drop per unit lenght for the conductor i can be defined from the source current density J_{si} as

$$V_i = J_{si} / \sigma \tag{25}$$

The corresponding impedance per unit lenght is

$$Z_i = V_i / I_{rms} \tag{26}$$

The real part of Z_i will be the ac resistance of conductor i, i.e.

$$R_{ac\ i} = Z_{i\ real} \tag{27}$$

so the three conductors will have a total ac resistance

$$R_{ac} = (R_{ac1} + R_{ac2} + R_{ac3}) / 3 \tag{28a}$$

or in the symmetrical case

$$R_{ac} = R_{ac\ i}\ ,\quad i = 1, 2, 3 \quad . \tag{28b}$$

For the evaluation of the quantities in the right side of (24) let us examine a typical element e that lies on the cross-section of the conductor i, as shown in Fig.2. The element is a first-order triangle with local nodes numbered from 1 to 3 and mid-side nodes numbered from 4 to 6. The nodal potential values A^e_1, A^e_2 and A^e_3 and the source current density J_{si} of the conductor i are known from the solution of (20).

From the definition of J_e (15) the relation between $A^e_e(x, y)$ and $J^e_e(x, y)$, i.e. for the typical element e, will be

$$J^e_{e\ i}(x, y) = -j\omega\sigma A^e(x, y) \tag{29}$$

and the total current density distribution of element e can be obtained from

$$J^e_i(x, y) = J^e_{e\ i}(x, y) + J_{si} \quad . \tag{30}$$

The eddy current I^e_e of the element e can be computed from

$$I^e_{e\ i} = \iint_{S^e} I_{e\ i}(x, y)\, dxdy \quad . \tag{31}$$

The integral in (31) can be expressed using symmetric quadrature formulae [6] of first degree, so

$$I^e_{e\ i} = -j\omega\sigma \frac{S^e}{3}(A^e_1 + A^e_2 + A^e_3) \tag{32}$$

while the source current I^e_s of the element e is

$$I^e_{s\ i} = J_{s\ i}\, S^e \tag{33}$$

and the total element current I^e_i is

$$I^e_i = I^e_{e\ i} + I^e_{s\ i} \quad . \tag{34}$$

The average loss density (W/m^3) contribution of element e is given by

$$U^e(x, y) = J^e(x, y)\, J^{e*}(x, y) / \sigma \tag{35}$$

and the losses per unit lenght will be

$$P^e = \iint_{S^e} U^e(x, y)\, dxdy \quad . \tag{36}$$

The integral in (36) can be expressed using symmetric quadrature formulae of second degree, so

$$P^e_{ci} = \frac{S^e}{3}(|J_{si} - j\omega\sigma A_4|^2 + |J_{si} - j\omega\sigma A_5|^2 + |J_{si} - j\omega\sigma A_6|^2) \quad . \tag{37}$$

Because of the linearity of the interpolation functions N(x, y) (see Appendix I) the mid-side vector potential values are

$$\begin{aligned} A^e_4 &= (A^e_1 + A^e_2) / 2 \\ A^e_5 &= (A^e_2 + A^e_3) / 2 \\ A^e_6 &= (A^e_3 + A^e_1) / 2 \quad . \end{aligned} \tag{38}$$

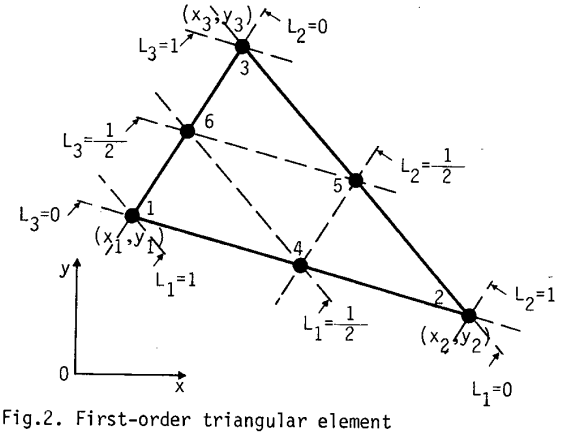

Fig.2. First-order triangular element

If the typical element e is not on a conductor but on the sheath cross-section, the source current density will be equal to zero because the sheath carries no source current but only induced eddy currents. So (37) changes to

$$P_s^e = \omega^2 \sigma \frac{S^e}{3} (|A_4^e|^2 + |A_5^e|^2 + |A_6^e|^2) \quad . \tag{39}$$

The total loss per unit length of conductor i is obtained from the summation of the element loss contributions of this conductor

$$P_{ci} = \sum_e P_{ci}^e \quad , \qquad i = 1, 2, 3 \tag{40}$$

and the total loss per unit length in the sheath

$$P_s = \sum_e P_s^e \tag{41}$$

where now the summation is over the elements of the sheath.

In the same way the total conductor current is given by

$$I_i = \sum_e I_i^e \quad , \quad i = 1, 2, 3 \tag{42}$$

It is easy to verify this result with the values given in (1).

6. Inductances

The skin and proximity effects and the presence of the sheath reduce the flux-carrying capacity of the three conductors and therefore reduce their inductance. The total impedance per unit length of conductor i is given by (26) and the reactance per unit length is the imaginary part of Z_i, i.e.

$$X_i = Z_{i\ imag} \tag{43}$$

and the inductance per unit length is

$$L_{ci} = X_i / \omega \tag{44}$$

The conductor inductances can be also obtained from the evaluation of the stored magnetic energy, given by

$$W = \frac{1}{2} \iiint_V \vec{J} \cdot \vec{A}\, dV \quad . \tag{45}$$

The mean value of this energy per unit length of conductor i is given by

$$W_{mi} = Re\left\{\frac{1}{2} \iint_{S_i} A(x,y) J^*(x,y)\, dxdy\right\} \tag{46}$$

and after separating J(x,y) with the help of (13), W_{mi} becomes

$$W_{mi} = \frac{1}{2} Re\left\{J_s^* \iint_{Si} A(x,y)\, dxdy\right\} \quad . \tag{47}$$

The stored magnetic energy is connected through L_{ci} with the relation

$$W_{mi} = \frac{1}{2} L_{ci} I_{rms}^2 \tag{48}$$

and the inductance can be calculated from

$$L_{ci} = \frac{1}{I_{rms}^2} Re\left\{J_s^* \iint_{S_i} A(x,y)\, dxdy\right\} \tag{49}$$

If we consider the inductance per phase of a symmetrical arrangement consisting of three solid circular conductors with radius r_a being at a distance m and without a sheath

$$L_s = \frac{\mu_o}{2\pi} \left(\ln \frac{m}{r_a} + \frac{1}{4}\right) \tag{50}$$

as a base inductance, we can have a relative-magnitude information of the operational inductance examining the ratios L_{ci}/L_s.

7. Forces

The force per volume element of a conductor in which the current density is $\vec{J}$ is given by the Lorenz relation

$$\vec{F} = \vec{J} \times \vec{B}$$

Because we have assumed that the problem is a two-dimensional one, we shall have $\vec{J} = \hat{z}J$ and $\vec{B} = \hat{x}B_x + \hat{y}B_y$. The force per unit length of each conductor's element will be given by

$$\vec{F}^e = \hat{x}\, F_x^e + \hat{y}\, F_x^e \tag{51a}$$

where

$$F_x^e = -\iint_{S^e} J^e(x,y) B_y^e\, dxdy$$

$$F_y^e = \iint_{S^e} J^e(x,y) B_x^e\, dxdy \tag{51b}$$

It can be shown using (31) that the time functions f_x and f_y will be obtained as (see Appendix II)

$$\begin{aligned} f_x^e(t) &= -I_{rms}^e B_{y\ rms}^e \cos(\theta^e - \varphi_y^e) + \cos(2\omega t + \theta^e + \varphi_y^e) \\ f_y^e(t) &= I_{rms}^e B_{x\ rms}^e \cos(\theta^e - \varphi_x^e) + \cos(2\omega t + \theta^e + \varphi_x^e) \end{aligned} \tag{52}$$

Finally the total force functions will be derived from the summation of the element contributions of this conductor

$$\begin{aligned} f_x(t) &= \sum_e f_x^e(t) \\ f_y(t) &= \sum_e f_y^e(t) \end{aligned} \tag{53}$$

and the total force vector will be

$$\vec{f}(t) = \hat{x}\, f_x(t) + \hat{y}\, f_y(t) \tag{54}$$

Using the expressions in (52), the force components will be obtained as

$$\begin{aligned} f_x(t) &= -\alpha_x \left[\beta_x + \cos(2\omega t + \gamma_x)\right] \\ f_y(t) &= \alpha_y \left[\beta_y + \cos(2\omega t + \gamma_y)\right] \end{aligned} \tag{55a}$$

where

$$\begin{aligned} \alpha_x &= \Sigma_{x1} + \Sigma_{x2} & \alpha_y &= \Sigma_{y1} + \Sigma_{y2} \\ \beta_x &= \Sigma_{xo} / \alpha_x & \beta_y &= \Sigma_{yo} / \alpha_x \\ \gamma_x &= \tan^{-1}\left(\Sigma_{x1}/\Sigma_{x2}\right) & \gamma_y &= \tan^{-1}\left(\Sigma_{y1}/\Sigma_{y2}\right) \end{aligned} \tag{55b}$$

and

$$\Sigma_{xo}=\sum_e f^e_{xo}\cos(\theta-\varphi_y) \qquad \Sigma_{yo}=\sum_e f^e_{yo}\cos(\theta-\varphi_x)$$

$$\Sigma_{x1}=\sum_e f^e_{xo}\sin(\theta+\varphi_y) \qquad \Sigma_{y1}=\sum_e f^e_{yo}\sin(\theta\ \varphi_x) \qquad (55c)$$

$$\Sigma_{x2}=\sum_e f^e_{xo}\cos(\theta+\varphi_y) \qquad \Sigma_{y2}=\sum_e f^e_{yo}\cos(\theta+\varphi_x)$$

$$f^e_{xo}=I^e_{rms}B^e_{y\ rms} \qquad f^e_{yo}=I^e_{rms}B^e_{x\ rms} \ .$$

It can be shown that the locus of the force vector in (54) for a time variation equal to the half period is a real ellipse with center at the point

$$f_{xc} = -\alpha_x\beta_x$$

$$f_{yc} = \alpha_y\beta_y \ . \qquad (56)$$

The forces are related to the force f_b which applies between two straight parallel conductors carrying a current I_{rms} and being at a distance $m/\sqrt{3}$ apart

$$f_b = \frac{\mu I^2_{rms}}{2\pi m/\sqrt{3}} \ . \qquad (57)$$

8. Flux and current density distribution

It is well known that for a two-dimensional problem the curves A=constant are the lines of the flux density. The approximation (18) for the vector potential is linear, so that the flux density whithin each element will be constant. Such vector equipotentials, formed from line segments inside each element, have been plotted for uniform increments bound flux tubes containing the same flux.

A real function $a^e(x,y,t)$ for the vector potential in the element e can be obtained (see Appendix II) and this allows the calculation and plotting of the flux lines for any given time and not only at the time where the current is at its maximum or minimum value.

The current density distribution in the conductors can be obtained from (30). The sheath has no source current and therefore the current density for a sheath's element will be obtained from (29).

9. Results

A three phase gas cable has been considered with geometry given by

$$R_i = 15 \text{ in} = 0.381 \text{ m} \ ,$$

$$d_c = 0.5 \text{ in} = 0.0127 \text{ m} \ ,$$

$$\frac{m}{\sqrt{3}R_i} = 0.51 \ , \quad \frac{r_a}{R_i} = 0.18$$

and physical properties

$$\mu_{rc} = 1 \ ,$$

$$\sigma_c = 2.725\cdot10^7/\Omega m \ ,$$

$$\sigma_s = 2.875\cdot10^6/\Omega m \ .$$

The power loss ratio of the sheath was calculated as a function of relative permeability μ_{rs}, for three different wall thicknesses d_s. Comparison of the results obtained in this paper with those obtained in Fig.5 of [1] and in Fig.4 of [2] is presented in Fig.3. It can be seen that the wall thickness is an important parameter and the assumption of a sheath filling all of the outside space (i.e. infinite wall thickness d_s) may lead to an underestimation of the losses, when

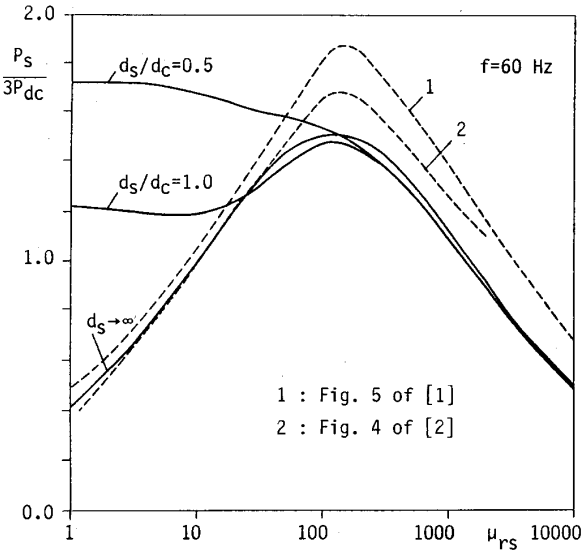

Fig.3. Comparison of sheath losses calculated with finite element method (solid lines) and with approximating models (dashed lines)

$d_s/\delta_s<1$. This is the case where the eddy currents in the sheath are restricted by lack of space (resistance-limited) and happens when $\mu_{rs}<40$ for the case with $d_s/d_s=0.5$ and when $\mu_{rs}<10$ for the case with $d_s/d_c=1.0$. When $d_s/\delta_s>1$ the extent of the current density distribution is limited by the effect of its own field (inductance-limited). It can be seen that the assumption of line conductors with uniform current density (ignoring the skin and proximity effects) may now lead to an overestimation of sheath's losses. This was also expected, because the current density in the conductors is maximum on the sides facing the centre of the cable, so that the induced eddy currents in the sheath (and also the losses) are lower.

The maximum losses in the case $d_s/\delta_s=1.0$ appears when $\mu_{rs}=150$. Taking this point as a reference, a non-symmetrical conductor arrangement has been examined. The phase conductor #1 has been moved in the x- and y-directions (as shown in Fig.1) and the losses, inductances and forces have been calculated. The displacements m_x and m_y from the original symmetrical position are related to the conductor radius r_a in order to have a relative information about the position of this conductor.

In Fig.4 the loss ratios defined in (24a) are shown vs the x-direction ratio m_x/r_a. Taking as a reference the losses in the symmetrical position (when $m_x/r_a=0.0$), the sheath losses vary from -27% (when $m_x/r_a=-1.0$) to 37% (when $m_x/r_a=1.0$) while the losses of the phase conductors vary up to 8%.

In Fig.5 the inductances of the three phase conductors related to the inductance L_s defined in (50) are shown vs the ratio m_x/r_a. The inductance L_{c1} of conductor #1 varies from -16% (when $m_x/r_a=-1.0$) to 12% (when $m_x/r_a=1.0$), taking as a reference the inductance of this conductor in the symmetrical position.

In Fig.6 the forces acting on the three conductors vs ratio m_x/r_a are shown. The forces are related to the force f_b defined in (57) and they are plotted for a time variation equal to a half period. It can be seen that the outward force acting on conductors #2 and #3 increases when conductor #1 is moving to the center of the cable while the contrary seems to happen on conductor #1. The center of the ellipses defined in (56) follow the movement of conductor #1.

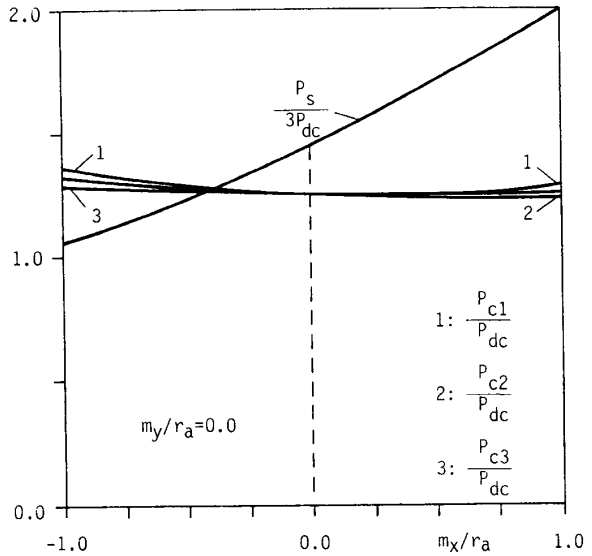

Fig.4. Sheath and conductor losses vs conductor #1 x-direction displacement

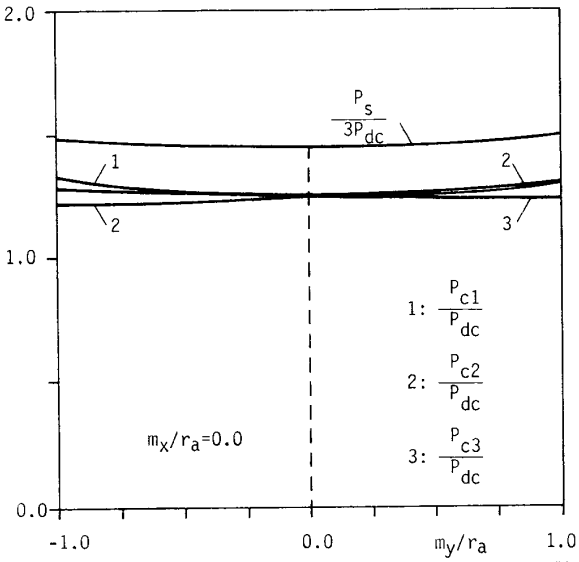

Fig.7. Sheath and conductor losses vs conductor #1 y-direction displacement

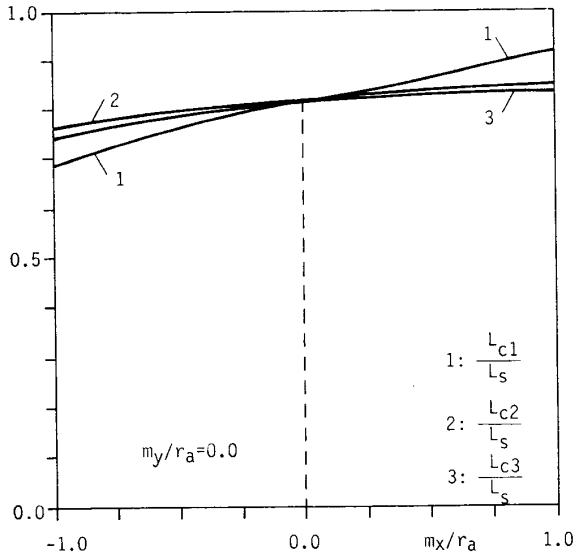

Fig.5. Conductor inductances vs conductor #1 x-direction displacement

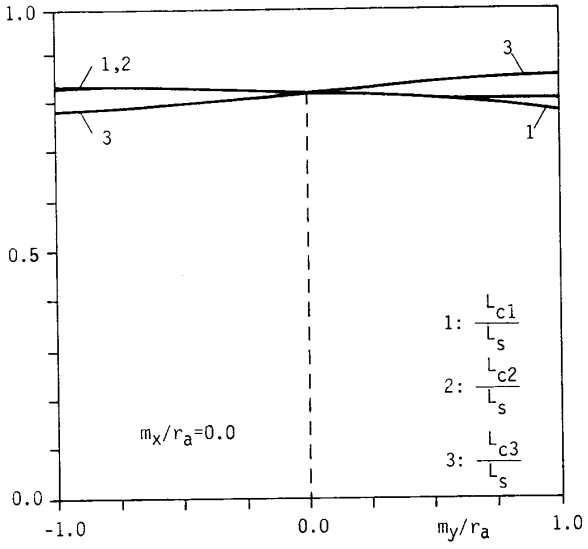

Fig.8. Conductor inductances vs conductor #1 y-direction displacement

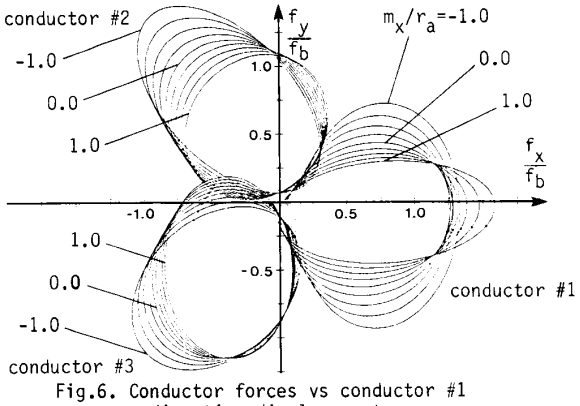

Fig.6. Conductor forces vs conductor #1 x-direction displacement

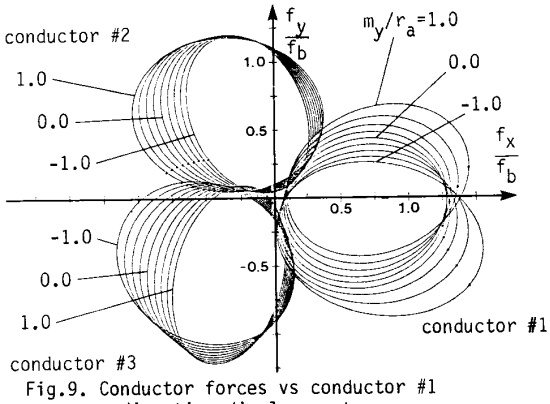

Fig.9. Conductor forces vs conductor #1 y-direction displacement

In Fig.7, 8 and 9 the losses, inductances and forces vs the y-direction displacement are shown. It can be seen that the effect of the y-direction displacement of conductor #1 on the losses and inductances is small, but the forces acting on the three conductors vary considerably.

In Fig.10 the magnetic vector equipotentials are plotted in the case with asymmetry of conductor #1 given by $m_x/r_a=1.0$ and $m_y/r_a=0.0$ (when the losses are higher). The plots have been made for four different times ($\omega t=0^0$, 30^0,60^0 and 90^0) and with a constant potential increment equal to $0.08\cdot10^{-3}$ Wb/m.

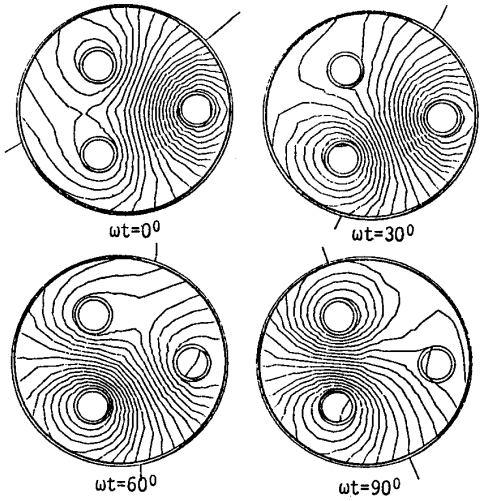

Fig.10. Magnetic vector equipotentials with asymmetry of conductor #1 given by $m_x/r_a=1.0$ and $m_y/r_a=0.0$

The validity of the finite element method was confirmed for the symmetrical case by comparing in detail with the results of the analytical solution [4] and with the measured data given in Table I of [7] . In both cases the agreement was excellent and the differences were between 0% and 4%.

10. Conclusions

The finite element procedure that treats the source current density as an unknown leads to valuable and accurate solutions of the steady-state field problem in a three-phase cable, taking into account the real geometry and assuming linearity. There are no other restrictions like asymmetry in the load currents or in the geometry.

Current densities, losses, inductances and forces can be calculated. Comparisons with published theoretical and experimental results, concerning the symmetrical case, give a satisfactory agreement. A non-symmetrical conductor arrangement leads to significant changes in the losses and forces.

APPENDIX I
Basic formulae for first-order triangular elements

Consider the typical first-order triangular element e shown in Fig.2, with local potential nodal values

$$\mathbf{A}^e = \begin{bmatrix} A_1^e \\ A_2^e \\ A_3^e \end{bmatrix}$$

Using the first-order shape functions

$$\mathbf{N}^e(x,y) = \frac{1}{2S^e}\begin{bmatrix} a_1+b_1x+c_1y \\ a_2+b_2x+c_2y \\ a_3+b_3x+c_3y \end{bmatrix}$$

where the coefficients a_i, b_i and c_i are well known from the literature [11] and S^e the area of element e, we shall have the space approximation of the vector potential as a phasor

$$A^e(x,y)=\mathbf{N}^{eT}\mathbf{A}^e=A_{real}(x,y)+jA_{imag}(x,y) \qquad (A1)$$

Suppose the element e lies on the conductor i, at which the sourse current density is J_{si}. Because J_{si} is a constant over the cross-section of this conductor, the phasor of the element e source current density will be

$$J_s^e = J_{si} \qquad (A2)$$

Assembling the element contributions over the whole domain,the space approximation for the vector potential will be obtained as in (18a). Likewise, assembling the conductor contributions the space approximation for the source current density will be obtained as in (18b).

Using the well-known [11] local area coordinate system for the first-order triangle L_1, L_2 and L_3, is easy to see that the area coordinates for the midside nodes 4,5 and 6 are (1/2, 1/2,0), (0,1/2,1/2) and (1/2, 0,1/2) respectively. According to the relation between L_i and $N_i^e(x,y)$

$$L_i = N_i^e(x,y) \quad , \quad i = 1,2,3$$

is easy to verify the relations (38).

APPENDIX II
Relations between phasors and real functions

The complex function

$$\tilde{A}(t) = \sqrt{2}\, A_{rms}\, e^{j(\omega t+\alpha)} \qquad (A3)$$

is related with a phasor

$$A = A_{rms}\, e^{j\alpha} = A_{real} + jA_{imag} \qquad (A4)$$

and with a real function of time

$$a(t) = Re\left\{\tilde{A}(t)\right\} = Re\left\{\sqrt{2}Ae^{j(\omega t+\alpha)}\right\}$$
$$= \sqrt{2}\, A_{rms}\cos(\omega t+\alpha) \qquad (A5)$$

The product of two real functions of time is

$$a(t)b(t) = Re\left\{A\,B^*\right\}+Re\left\{A\,B\,e^{j2\omega t}\right\} =$$
$$= A_{rms}B_{rms}\left[\cos(\alpha-\beta)+\cos(2\omega t+\alpha+\beta)\right] \qquad (A6)$$

and the mean value of this product is

$$\langle a(t)b(t)\rangle = Re\left\{A\,B^*\right\} =$$
$$= A_{rms}B_{rms}\cos(\alpha-\beta) \qquad (A7)$$

If we consider the typical element e in Fig.2 with the nodal potential value

$$A_m = A_{m\ real} + jA_{m\ imag} \ , \ m = 1,2,3$$

the corresponding real function of time will be

$$a_m(t)=\sqrt{2}\, A_{m\ rms}\cos(\omega t+\alpha_m) \qquad (A8)$$

where $A_{m\ rms} = \left[\left(A_{m\ real}\right)^2 + \left(A_{m\ imag}\right)^2\right]^{\frac{1}{2}}$

and $\alpha_m = \tan^{-1}\left(A_{m\ imag}/A_{m\ real}\right)$

Likewise the phasors for the total element current I^e and for the flux density components B^e_x and B^e_y will be

$$I^e = I^e_{rms}\, e^{j\theta^e} \qquad \text{(A9a)}$$

$$B^e_x = B^e_{x\ rms}\, e^{j\varphi^e_x} \qquad \text{(A9b)}$$

$$B^e_y = B^e_{y\ rms}\, e^{j\varphi^e_y} \qquad \text{(A9c)}$$

and the products of the corresponding time functions with the help of (A6) will give the force relations in (52).

Finally the space-time real function of the vector potential in the element e will be obtained from (A1) and (A8) as

$$a^e(x,y,t)=\sqrt{2}\, A^e_{rms}(x,y)\, \cos\left[\omega t+\alpha^e(x,y)\right] \qquad \text{(A10)}$$

where

$$A^e_{rms}(x,y)=\left[\left(A^e_{real}(x,y)\right)^2+\left(A^e_{imag}(x,y)\right)^2\right]^{\frac{1}{2}}$$

and

$$\alpha^e(x,y) = \tan^{-1}\left(A_{imag}(x,y)/A_{real}(x,y)\right)$$

Glossary of symbols

A	: magnetic vector potential (Wb/m)
d_c, d_s	: thicknesses of conductor and sheath wall respectively (m)
δ_s	: skin depth of sheath (m)
e (superscript)	: element
f_x, f_y	: x and y components of the force per unit length acting on a conductor (N/m)
f	: frequency (Hz)
j	: imaginary unit
J_e, J_s	: eddy current density and source current density respectively (A/m^2)
L_{ci}	: inductance per unit length of conductor i (H/m)
L_i	: area coordinate of local node i
m	: distance between conductor centers in the symmetrical case (m)
m_x, m_y	: x and y direction displacements of conductor #1 from the symmetrical position (m)
μ_{rc}, μ_{rs}	: relative permeability of conductors and sheath respectively
P_{dc}	: dc loss per unit length of a conductor (W/m)
P_{ci}, P_s	: ac loss per unit length of conductor i and sheath respectively (W/m)
r_a	: outside radius of conductors (m)
R_{ac}	: ac resistance per unit length of the three phase cable (Ω/m)
R_{dc}	: dc resistance per unit length of a conductor (Ω/m)
R_i	: inside radius of the sheath (m)
σ_c, σ_s	: conductivities of conductors and sheath respectively (1/Ωm)
T (superscript)	: transposed (matrix or vector)
$\hat{x}, \hat{y}, \hat{z}$	: unit vectors in a Cartesian coordinate system

REFERENCES

1) A.Emanuel and H.C.Doepken, "Calculation of losses in steel enclosures of three phase bus or cables", IEEE Transactions on Power Apparatus and Systems, vol. PAS-93, pp. 1758-1767, 1974.
2) R.Sikora, J.Purczynski, R.Pazka and S.Gratkowski, "Analysis of electromagnetic field and power losses in three phase gas insulated cable", IEEE Transactions on Magnetics, vol. MAG-13, pp. 1140-1142, September 1977.
3) D.Tampakis and P.Dokopoulos, "Eddy currents and forces in a three phase gas insulated cable with steel enclosure", IEEE Transactions on Magnetics, vol. MAG-19, pp. 2210-2212, September 1983.
4) D.Tampakis and P.Dokopoulos, "Analysis of field and losses in a three phase gas cable with thick walls Part II: Calculation of losses and results", IEEE Transactions on Power Apparatus and Systems, vol. PAS-104, pp. 9-15, January 1985.
5) J.Weiss and Z.J.Csendes, "A one-step finite element method for multiconductor skin effect problems", IEEE Transactions on Power Apparatus and Systems , vol. PAS-101, pp.3796-3803, October 1982.
6) P.Silvester, "Symmetric quadrature formulae for simplexes", Mathematics of Computation, vol. 24 , no. 109, pp.95-100, January 1970.
7) P.C.Bolin, A.H.Cookson et al, "Manufacture and installation of a three conductor SF_6 insulated transmission line", IEEE Transactions on Power Apparatus and Systems, vol.PAS-101, pp.1966-1974, July 1982.
8) A.Konrad, "Integrodifferential finite element formulation of two-dimensional steady-state skin effect problems", IEEE Transactions on Magnetics, vol. MAG-18, pp. 284-292, January 1982.
9) G.Strang, Linear algebra and its applications, Florida:Academic Press, 1984, pp.19-26.
10) P.Silvester and R.Ferrari, Finite element for electrical engineers, Cambridge: Cambridge University Press, 1983, pp. 79-80.
11) O.C.Zienkiewicz, The finite element method, New York: McGraw-Hill, 1977, pp.164-168.

BIOGRAPHIES

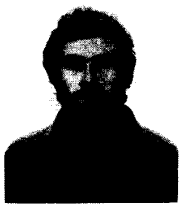

Dimitris Labridis was born in Thessaloniki, Greece on July 26, 1958. He received his Dipl.-Eng. degree from the Department of Electrical Engineering at the Aristotelian University of Thessaloniki, Greece in November 1981.

Since 1982 he has been working as a research assistant at the Department of Electrical Engineering at the Aristotelian University of Thessaloniki, Greece. His special interests are power system analysis with special emphasis on the simulation of transmission systems and electromagnetic field analysis.

He is a member of Eta Kappa Nu.

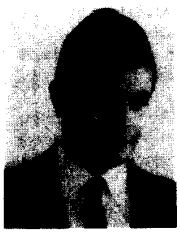

Petros Dokopoulos (M'74) was born in Athens, Greece on September 16, 1939. He received his Dipl.-Eng. degree from the Technical University of Athens in July 1962 and his Ph.D degree from the University of Brunswick, FRG, in 1967.

He was 1962-1967 with the High Voltage Laboratory at the University of Brunswick, FRG, 1967-1974 with the Nuclear Research Center at Jülich, FRG and 1974-1978 with the Joint European Torus.Since 1978 he is full professor at the Department of Electrical Engineering at the Aristotelian University of Thessaloniki, Greece. He has worked as consultant to Brown Boveri and Cie, Mannheim, to Siemens, Erlangen, to Public Power Corporation, Greece and to National Telecommunication Organization, Greece.

His scientific fields of interest are dielectrics, power switches, generators, power cables and alternative energy sources. He has 41 publications and seven patents on these subjects.